
Dual RNA-seq analysis pinpoints to a balanced regulation between symbiosis and immunity in the *Medicago truncatula*-*Sinorhizobium meliloti* symbiotic interactions

Dandan Zhang , Qiujin Wu , Yanwen Zhao , Ziang Yan , Aifang Xiao , [Haixiang Yu](#) * , [Yangrong Cao](#) *

Posted Date: 11 September 2023

doi: 10.20944/preprints202309.0662.v1

Keywords: legume-rhizobial symbiosis; *Medicago truncatula*; *Sinorhizobium meliloti*; NAD1; defense; Dual RNA-seq



Preprints.org is a free multidiscipline platform providing preprint service that is dedicated to making early versions of research outputs permanently available and citable. Preprints posted at Preprints.org appear in Web of Science, Crossref, Google Scholar, Scilit, Europe PMC.

Copyright: This is an open access article distributed under the Creative Commons Attribution License which permits unrestricted use, distribution, and reproduction in any medium, provided the original work is properly cited.

Article

Dual RNA-Seq Analysis Pinpoints to a Balanced Regulation between Symbiosis and Immunity in the *Medicago truncatula*-*Sinorhizobium meliloti* Symbiotic Interactions

Dandan Zhang ¹, Qiujiu Wu ¹, Yanwen Zhao ¹, Ziang Yan ¹, Aifang Xiao ¹, Haixiang Yu ^{1,*} and Yangrong Cao ^{1*}

¹ National Key Laboratory of Agricultural Microbiology, College of Life Science and Technology, Huazhong Agricultural University, Wuhan, Hubei, 430070, China; zdd0103@webmail.hzau.edu.cn (D.Z.); 15196882085@163.com (Q.W.); 18939415287@163.com (Y.Z.); 1532444096@qq.com (Z.Y.); 81899150@qq.com (A.X.).

* Correspondence: yrcao@mail.hzau.edu.cn (Y.C.); yseaflying@mail.hzau.edu.cn (H.Y.)

Abstract: Legume-rhizobial symbiosis leads to the formation of root nodules, where rhizobia reside and develop into bacteroids to reduce nitrogen into ammonium for plant growth, which leaves an opening question as how plant immunity is attenuated in nodules in the presence of large number of foreign bacteria. In *Medicago truncatula*, mutation in *NAD1* (Nodules with Activated Defense 1) only produces necrotic nodules with overactivated immunity, indicating *NAD1* is an indispensable component required for suppressing immunity in nodules. In this study, a dual RNA-seq transcriptomic technology was performed to extensively analyze gene expressions in *nad1-1* mutant nodules. We identified 89 DEGs in symbiotic nitrogen fixation and 89 DEGs in immunity in *Medicago truncatula* at 10 dpi. Simultaneously, we identified 27 DEGs in *fix* and *nif* genes in *Sinorhizobium meliloti*. Then we identified 56 DEGs related to stress, including ROS, NO, and NCR, most of which were upregulated in *Sinorhizobium meliloti*. Our analyses of nitrogen fixation-defective plant *nad1-1* mutants with overactivated defense indicate that host use plant immunity to control massive bacterial colonization during early and late symbiotic stages. Our findings provide insight into the function of *NAD1* in improvement or inhibition of plant immune response to maintain symbiosis during rhizobial endosymbiosis.

Keywords: legume-rhizobial symbiosis; *Medicago truncatula*; *Sinorhizobium meliloti*; *NAD1*; defense; dual RNA-seq

1. Introduction

Nitrogen is one of the main nutrient elements necessary for plant growth and development [1]. However, nitrogen in nature can only be absorbed by plant after it is reduced to be nitrate nitrogen or ammonia nitrogen [1]. Biological fixing nitrogen dominates in nitrogen reduction, and symbiotic fixing nitrogen is the most efficient biological fixing nitrogen method [2]. Rhizospheric nitrogen is formed by rhizobia and legumes [2]. Successful interactions between rhizobia and legume roots result in formation of a new organ, the root nodule, where rhizobia convert atmospheric nitrogen into organic nitrogen compounds to obtain the required carbon sources [2].

Legumes produce two major types of nodules, indeterminate and determinate nodules, which greatly differ in structure and metabolism [3]. The widely cultivated legumes with indeterminate nodules mainly include *Pisum sativum*, *Medicago truncatula*, *Trifolium repens*, and *Vicia faba*, whereas those with determinate nodules mainly include soybean, *Lotus japonicus*, *Phaseolus vulgaris*, and *Vigna unguiculata* [4]. The shape of indeterminate nodules is normal cylindrical or bifurcated, and the root nodule cells can be roughly divided into four zones according to the infection state of rhizobia: Zone

I is the meristem at the top of the root nodule; Zone II is the infection zone that releases rhizobia from the infection thread to infect plant cells; Zone II-III is the transition zone; Zone III is nitrogen fixation area; Zone IV is the senescent zone, where bacteroids are aging [5]. In the mature nodules, the central tissue containing nitrogen cells is uniform, including the cells infected by bacteroids and the uninfected cells [6,7]. After decay, nodules die radially from the center to the periphery, and bacteroids are released from the dead cells and become free bacteroids [5]. In addition to different nodule morphologies, the biggest difference between indeterminate and determinate nodules lies in that most of the rhizobia in indeterminate nodules undergo terminal differentiation including cell expansion, genome doubling, membrane modification, and loss of reproductive ability [8].

There is an exchange of chemical signals between plants and rhizobia throughout the different stages of nodule formation and development, which encompasses Nod factor signaling (NF signaling) as well as other plant signaling systems involving calcium, NADPH oxidase, and NO synthase systems. These systems, inducing alterations in gene expression within both partners, play a role in shaping partner selection and dampening plant defense [8,9]. These signals facilitate the entry of bacteria into plant epidermal and cortical cells, stimulate root cell division and the development of nodule meristem, leading to the formation of numerous specialized cellular organelles referred to as "symbiosomes", each housing one or more nitrogen-fixing bacteroids [9].

Microbe-associated molecular patterns (MAMPs) derived from pathogens can be recognized by pattern recognition receptors (PRRs) on plant cell membrane to trigger a variety of early defense reactions, including the production of a large number of reactive oxygen species (ROS) [10]. At present, the studies of PRRs mainly involve bacterial flagellin receptor FLAGELLIN SENSING 2 (FLS2) and chitin elicitor kinase (CERK1) [11,12]. In order to overcome the PAMP-triggered immune response (PTI), pathogens secrete effector proteins into plant cells through type III secretion system to inhibit plant immunity. Therefore, plants have evolved a variety of disease resistance (R) proteins to recognize effectors and produce effector-triggered immunity (ETI) [13]. Most of these R proteins belong to nucleoside binding site-leucine rich repeat (NBS-LRR). The activation of a large number of defense genes in ETI is often accompanied by hypersensitivity or hypersensitivity-like cell death and finally induces resistance to pathogen [14]. In fact, similar to pathogens invading host plants, rhizobia can induce innate immunity in plants when they contact roots of legume plants. However, this host defense response is transient, and it is inhibited during rhizobium invasion [15]. Symbiosis-induced immunosuppression is regulated by rhizobia or host plants in a variety of manners. Many evidences have indicated that rhizobia have evolved multiple strategies including ROS scavenging enzyme, nodulation factor (NF), lipopolysaccharide (LPS), extracellular polysaccharide (EPS), and type III/IV secretion system to escape or inhibit the immunity produced by the early symbiotic host [16–18]. In terms of host plants, multiple plant genes such as *DNF2* [19], *SymCRK* [20], *RSD* [21], and *NAD1* [22] have been found to be involved in immunosuppression in the late stage of symbiosis (the stage after the release of rhizobia into root nodule cells). Root nodules formed on mutant plants of these genes show defense-like responses [23]. Plant innate immunity plays an important role in regulating symbiotic processes of plants and rhizobia, including rhizobium infection, rhizobium colonization, and bacteroid differentiation in leguminous plants [24]. How to maintain rhizobial survival in plant cells without triggering defense responses remains largely unknown.

The transcriptional reprogramming in plant-microbe interaction leads to a particular cell fate for both bacteria and host plant [25,26]. By genome-wide transcription profiling, symbiosis-related plant and bacterial genes can be simultaneously identified before the bacteria are physically separated from host cells. In the previous research, the expression levels of bacterial genes and host plant genes were analyzed using transcription profiling, respectively [27,28]. So far, there have been no reports on the simultaneous analyses of gene expressions of both bacteria and hosts.

Therefore, this study adopted dual RNA-seq transcriptomics to analyze simultaneously gene expression changes in both symbiont and the host plant. We analyzed the interactions between rhizobia and host plant using immune defense-overactivated *nad1* mutant material at two developmental stages. We identified differentially expressed genes (DEGs) related to symbiosis regulation processes including NF signaling, nodule meristem and differentiation from both *M.*

truncatula and *S. meliloti*. This study made the first attempt to reveal dynamic balance between symbiosis and defense during bacterial endosymbiosis.

2. Results

2.1. Requirement of NAD1 for Nodule Development and Symbiotic Nitrogen Fixation

One previous study reported that the *nad1-1* mutant showed a significant nitrogen deficiency phenotype at 21 days post inoculation (dpi) with rhizobia. The *nad1-1* mutant grew shorter than the wild-type, exhibited yellowing, and formed more root nodules than the wild-type. The *nad1-1* mutant nodules were found to have no nitrogen fixation ability [22]. In this study, we investigated the early function of NAD1, and found that there was no significant difference between the *nad1-1* mutants and the wild-type at 6 dpi and 10 dpi in plant growth (Figure 1A). The number of root nodules in the *nad1-1* mutant showed no difference from that in the wild-type at 6 dpi, while it was slightly higher than that in the wild-type at 10 dpi (Figure 1B). Furthermore, the nitrogenase activity in *nad1-1* mutants was significantly lower than that in the wild-type at both 6 and 10 dpi, which is consistent with previous reports (Figure 1C) [22]. Compared to the absence of obvious brown pigments observed in the white nodules of the *nad1-1* nodules at 6dpi, significant deposition of severe brown pigments was detected in *nad1-1* nodules at 10dpi, in contrast to the pink nodules of the wild type (Figure 1D, 1E). This observation suggests visibly overactivated defense in *nad1-1* nodules at a later stage. At 6dpi, we observed abnormal infected cells with a reduced population of bacteria in Zone III of white nodules from the *nad1-1* nodules, in contrast to the pink nodules from the wild-type (Figure 1D). However, at 10 dpi, almost no complete symbiotic cells were observed in Zone III of the *nad1-1* nodules. Instead, bacteroids were released from the cells and accumulated in non-symbiotic intercellular spaces within the *nad1-1* mutant nodules (Figure 1E). Therefore, we examined transcriptomic analysis between the host and rhizobia during these two stages of nodules using dual RNA-seq approach to unravel the interaction between symbiosis and defense.

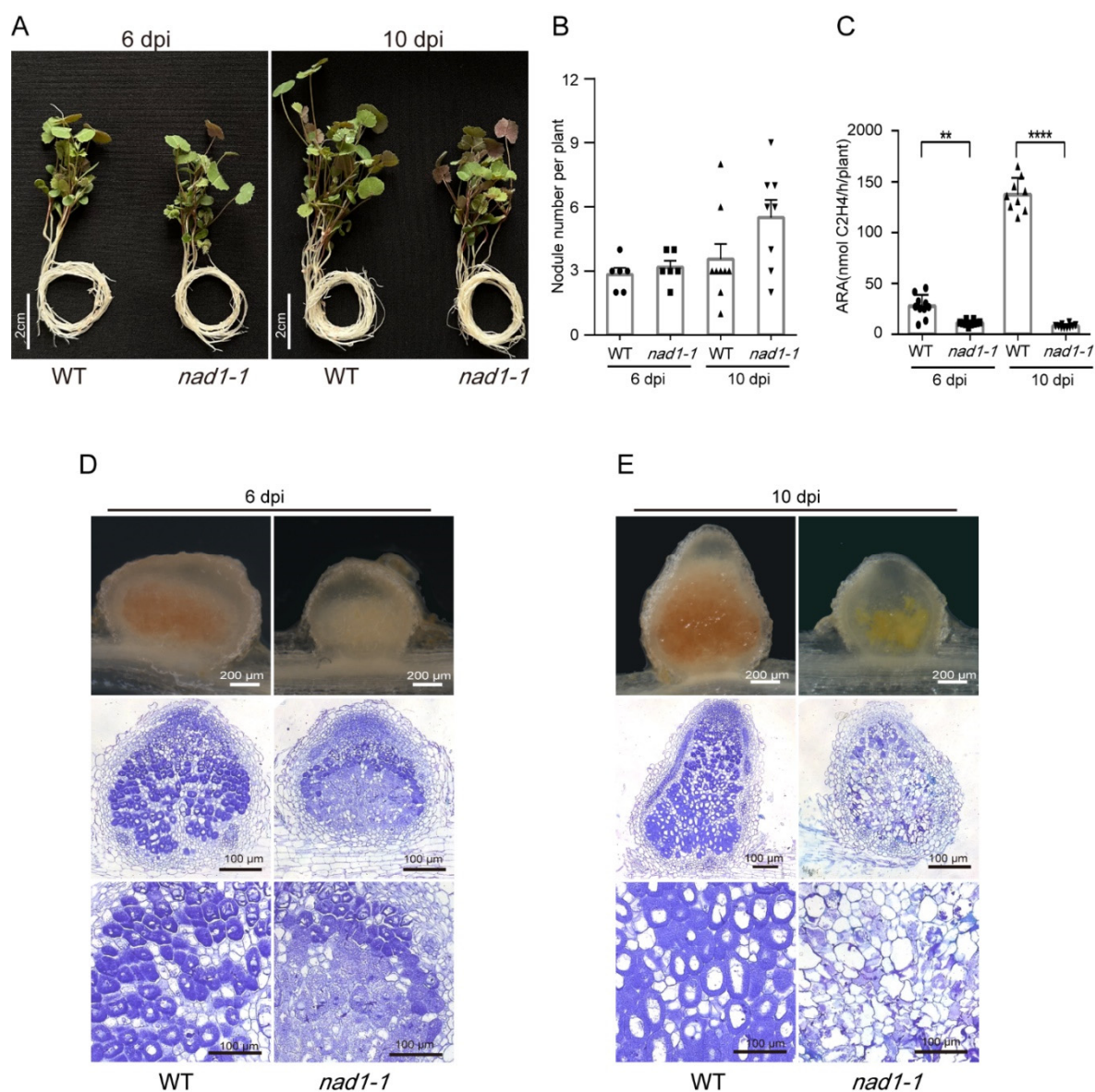


Figure 1. Phenotypes of the wild-type (WT) *Medicago truncatula* R108 and *nad1-1* mutant. A, Growth of WT and *nad1-1* at 6 d post inoculation (dpi) and 10 dpi inoculated with *Sinorhizobium meliloti* 2011. B, Nodule number per plant were measured at 6 dpi and 10 dpi. C, Acetylene reduction assay (ARA) reflecting nitrogenase activity was performed on nodulated plants. D and E, Sections of WT and *nad1-1* mutant nodules at 6 dpi and 10 dpi.

2.2. Identification of DEGs and function analysis in plant

Dual RNA-seq data revealed the differences in transcriptional signatures between different development stages of nodules (Figure 2A). According to the thresholds of $|\log_2 \text{FC}| > 1$, adjusted $p < 0.05$, we identified DEGs in the comparison of *nad1-1* mutants vs. wild-type (WT). A total of 936 plant DEGs were obtained (Table S1), of which 552 DEGs were upregulated and 384 DEGs were downregulated at 6dpi (Figure 2B). It should be noted that at 10 dpi, there was a dramatically increased number of DEGs (6598) (Table S1), of which 4107 DEGs were upregulated, and 2491 DEGs were downregulated (Figure 2B). Totally, 125 DEGs were shared by those identified at 6 dpi (936 DEGs) and 10 dpi (6598 DEGs) (Figure 2C). We defined these 125 shared DEGs in two stages as the “*nad1-1* signature”.

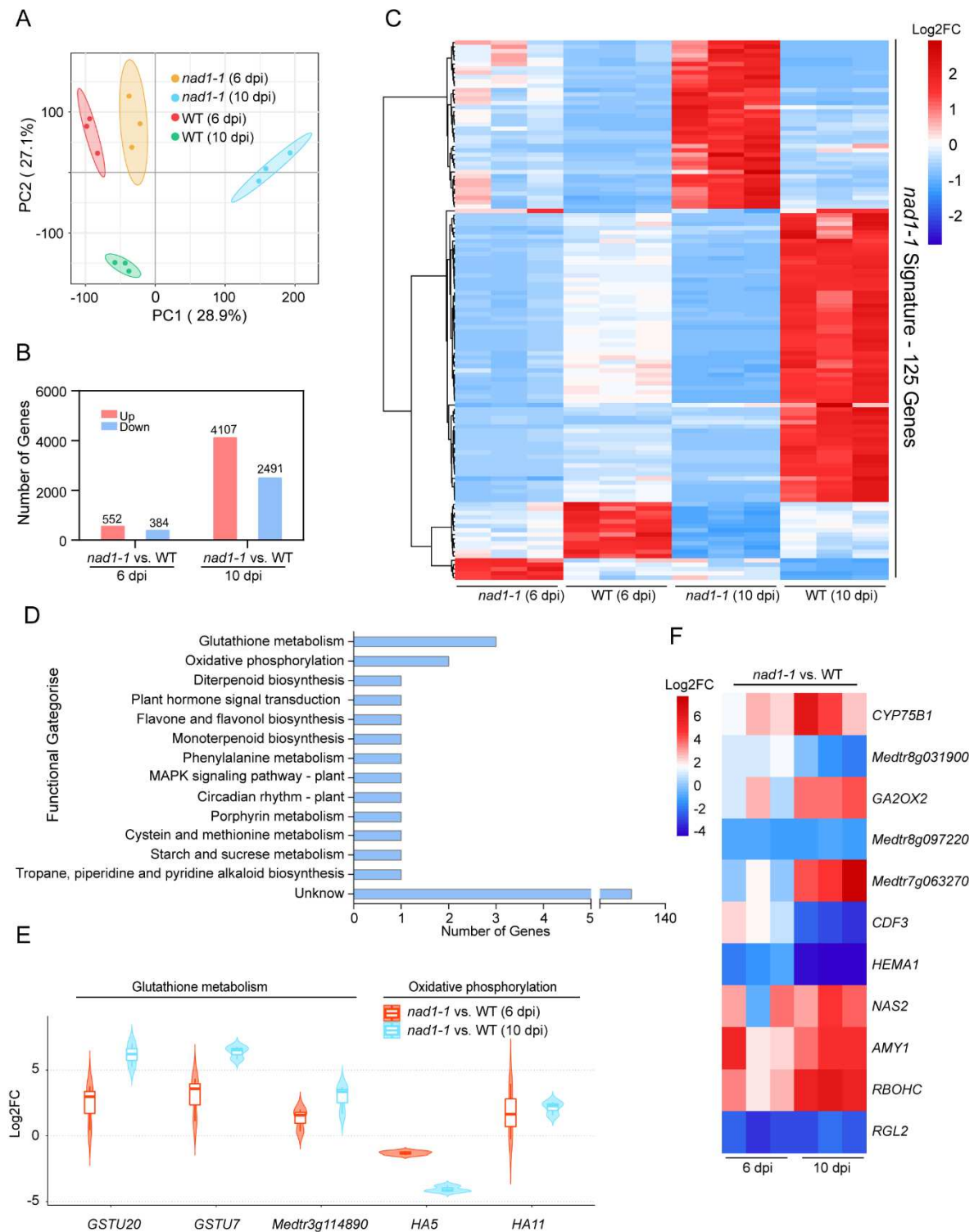


Figure 2. Identification of Signature genes in WT and *nad1-1* mutant. A, Principal-component analysis (PCA) of the WT and *nad1-1* transcriptome from two different times: *nad1-1* 6 dpi, wild-type (WT) 6 dpi, *nad1-1* 10 dpi, wild-type (WT) 10 dpi. B, Number of differentially expressed genes (DEGs) in *nad1-1* vs. WT at 6 dpi and 10 dpi. C, Heatmap showing relative expression levels for the "*nad1-1* signature," a set of 125 genes significantly regulated between *nad1-1* vs. WT at 6dpi,10dpi in *M. truncatula*. D, KEGG pathway enrichment analyses of the "*nad1-1* signature" genes. E, Violin plot showing expression levels of genes involved in the glutathione metabolism and oxidative phosphorylation pathways. F, Heatmap showing relative expression levels for the genes in the other pathways (D).

The functions of the “*nad1-1* signature” DEGs identified was investigated using KEGG pathway analysis (Figure 2D). The results showed that these “*nad1-1* signature” DEGs were mainly enriched in glutathione metabolism, oxidative phosphorylation, MAPK signaling pathway – plant, flavonoid and flavonoid biosynthetic pathways (Figure 2D). Notably, 3 “*nad1-1* signature” genes including *GSTU20* and *GSTU7* in the glutathione metabolism were significantly upregulated at 6dpi and 10 dpi (Figure 2E), suggesting that *GSTU20* and *GSTU7* were significantly accumulated to support rhizobium survival in nodules, which was consistent with genetic analysis results that these two genes participated in antioxidant reactions to eliminate the accumulation of ROS and lipid peroxides in infected tissues [29,30].

Plasma membrane H⁺-ATPase (P-type H⁺-ATPase) is a protein family of about 100kDa, which is considered as the exclusive protein of plant and fungal plasma membrane. This protein is localized on the biofilm to form an electrochemical gradient. P-type H⁺-ATPase can supply energy for metabolite absorption and responses to environment [31]. In our study, the *HA5* (one type of P-type H⁺-ATPase) was up-regulated, possibly providing energy for mutants to respond to rhizobial stress (Figure 2E).

Flavonoids are secondary metabolites widely distributed in plants. As a flavonoid 3'-hydroxylase, *CYP75B1* belongs to the cytochrome P450 monooxygenase family, and it participates in the flavonoid metabolic pathway [32]. More importantly, the expression of *CYP75B1* can induce flavonoid biosynthesis to regulate the ROS homeostasis [33]. In this study, among the regulated genes from 6 dpi and 10 dpi, *CYP75B1* was markedly up-regulated potentially to remove reactive oxygen species (ROS) so as to weaken the immune response caused by NAD1 protein deficiency in *nad1-1* mutant plant.

2.3. Identification of DEGs and their function analysis in rhizobia

We directly compared rhizobium RNA-seq profiles of two host rhizobium lineages *nad1-1* mutant and wild-type (WT) at 6 dpi and 10 dpi. PCA analysis of the rhizobium transcripts (Figure 3A) showed a very clear separation between *nad1-1* mutant and wild-type (WT) at 10 dpi, but no obvious separation at 6 dpi. A total of 661 rhizobial genes at 6 dpi (573 up-regulated, 88 down-regulated), were found to be differentially expressed ($|\log_2 \text{FC}| > 1$, adjusted $p < 0.05$) in comparison of *nad1-1* mutant vs. WT (Figure 3B, Table S2), while 2073 genes were differently expressed at 10 dpi, of which 1749 genes were up-regulated and 324 genes were down-regulated (Figure 3B, Table S2).

Totally, 25 rhizobial DEGs were shared at 6 dpi and 10 dpi, which defined as “rhizobium signature” (Figure 3C). Further, we performed KEGG pathway enrichment analysis of these rhizobium signature genes to reveal their functions. The results showed that 3 rhizobium signature genes were enriched in nitrogen metabolism, 2 in two-component system, and 1 in ABC transporters pathways during two stages of nodule development (6 and 10 dpi) (Figure 3D). The expression levels of 4 nitrogen fixation-related genes (*nifA*, *nifD*, *nifH*, and *nifK*) were significantly downregulated at both 6 and 10 dpi, which was consistent with the *nad1-1* mutant phenotypes of deficient nitrogen fixation nodule (Figure 3E,1B).

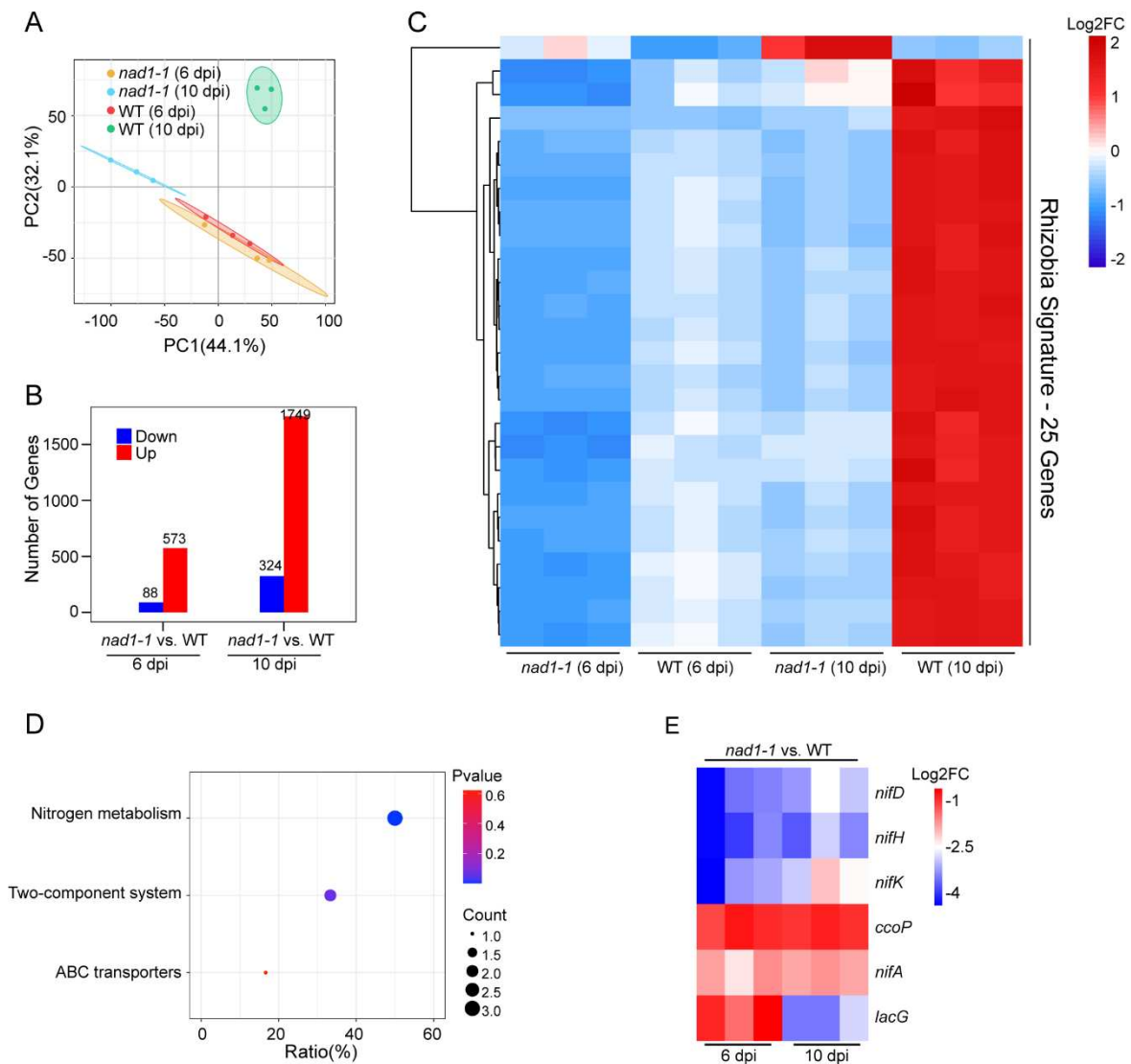


Figure 3. Analysis of different rhizobia transcriptional patterns in *nad1-1* vs. WT. A, Principal-component analysis (PCA) of the rhizobia transcriptome from two different times: *nad1-1* 6 dpi, wild-type (WT) 6 dpi, *nad1-1* 10 dpi, wild-type (WT) 10 dpi. B, Number of rhizobia differentially expressed genes (DEGs) in *nad1-1* vs. WT at 6 dpi and 10 dpi. C, Heatmap showing the relative expression levels of rhizobial genes for the “Rhizobia signature,” a set of 25 genes significantly regulated in *nad1-1* vs. WT at 6 dpi and 10 dpi. D, KEGG pathway enrichment analyses of the “Rhizobia signature” genes. E, Heatmap showing expression levels of genes involved in the nitrogen metabolism, two-component system and ABC transporter pathways.

2.4. Expression of genes associated with plant–rhizobia NF signaling process

Previous studies have demonstrated that NF signaling occurs not only in the nodule infection zone but also remains active in ZIII (the nitrogen-fixing zone), where it might be particularly associated with Its [35]. To investigate whether *NAD1* is involved in nodulation signaling, we investigate the expressions of nodulation signaling-related genes (Figure 4A, Table S3). The expression levels of early-stage nod factor (NF) signaling-related genes including *MtLYK3*, *MtNFP*, *MtDMI2*, *MtERN*, and *MtNSP2* exhibited no difference between *nad1-1* mutant and wild-type at 6 dpi or 10 dpi (Figure 4A), which suggested that *NAD1* may not involve in early-stage NF signaling and rhizobial infection. Root nodule development-related genes including *MtIPD3*, *MtDMI1*, *Apyrase-like*, *MtSYMREM*, and *MtPUB1* were down-regulated at 10 dpi (Figure 4B). LysM receptor *MtLYR4* and 3-Hydroxy-3-Methylglutaryl CoA Reductase 1 (*HMGR1*) showed little difference between *nad1-1* mutant and wildtype at 6 dpi, but their expression levels were significantly up-

regulated at 10 dpi (Figure 4B). Taken together, the expression levels of genes associated with NF signaling showed a significant change at 10 dpi. This is consistent with the phenotype observed in the nitrogen-fixing zone where a majority of cells have ruptured, as compared to the wild-type at the same 10 dpi point.

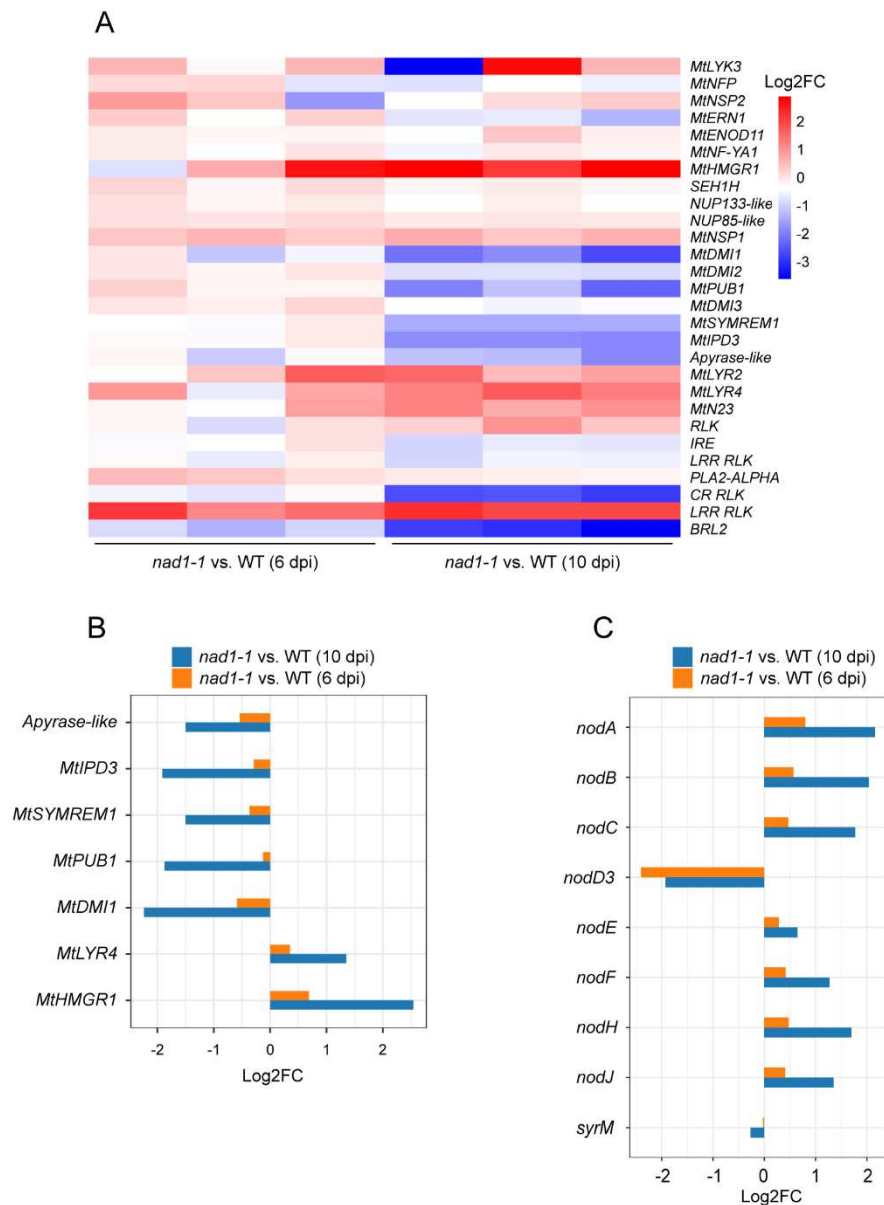


Figure 4. Candidate genes involved in the control of nod factor (NF) signaling. A, Heatmap showing the transcriptional expression levels of all plant genes related to nodule NF signaling. B, Barplot showing the expression levels of NF signaling-related genes regulated between *nad1-1* and WT at 6 dpi and 10 dpi in *M. truncatula*. C, Boxplot showing the expression levels of NF-genes regulated in *nad1-1* vs. WT at 6 dpi and 10 dpi in *S. meliloti*.

In terms of rhizobia, NF biosynthesis genes including *nodABC*, *nodF*, *nodH*, and *nodJ* exhibited little expression difference between *nad1-1* mutant and wild-type at 6dpi. However, their expression was significantly higher in *nad1-1* mutant than in wild-type at 10 dpi (Figure 4C, Table S4). The gene expression level of transcriptional regulator *nodD3* belonging to the LysR family [36] was significantly downregulated at both 6dpi and 10 dpi (Figure 4F). Instead, another transcriptional regulator, *SyrM*, activates *nodD3* expression [36], whose expression displayed no difference between *nad1-1* mutant and wild-type at either 6 dpi or 10 dpi (Figure 4C). These results indicated that *NAD1*

might play a role in the late stages of nodule development by affecting the expression level of root nodule-related genes.

2.5. Expression of genes involved in nodule meristem and differentiation

In order to determine *NAD1* whether played a role in nodule formation and development, we examined the expression levels of a series of genes related to nodule meristem and differentiation (Figure 5A, 5D, Table S5, S6) [35]. The results showed no significant difference in the expression of genes related to the nodule meristem and differentiation between *nad1-1* mutant and wild-type at 6dpi (Figure 5A, 5B), which implies that *NAD1* had no effect on nodule meristem and differentiation in the early stage. However, *SHY2* gene involved in cell differentiation was significantly upregulated at 10 dpi (Figure 5C). Moreover, two cell differentiation-promoting genes *MtCRE1* [37], cytokinin (CK) receptor gene, and *MtEFD* [38] encoding an APETALA2/ETHYLENE RESPONSIVE FACTOR (ERF) transcription factor in nodules were down-regulated at 10dpi (Figure 5C), which is consistent with arrested development of *nad1-1* nodules at late stage.

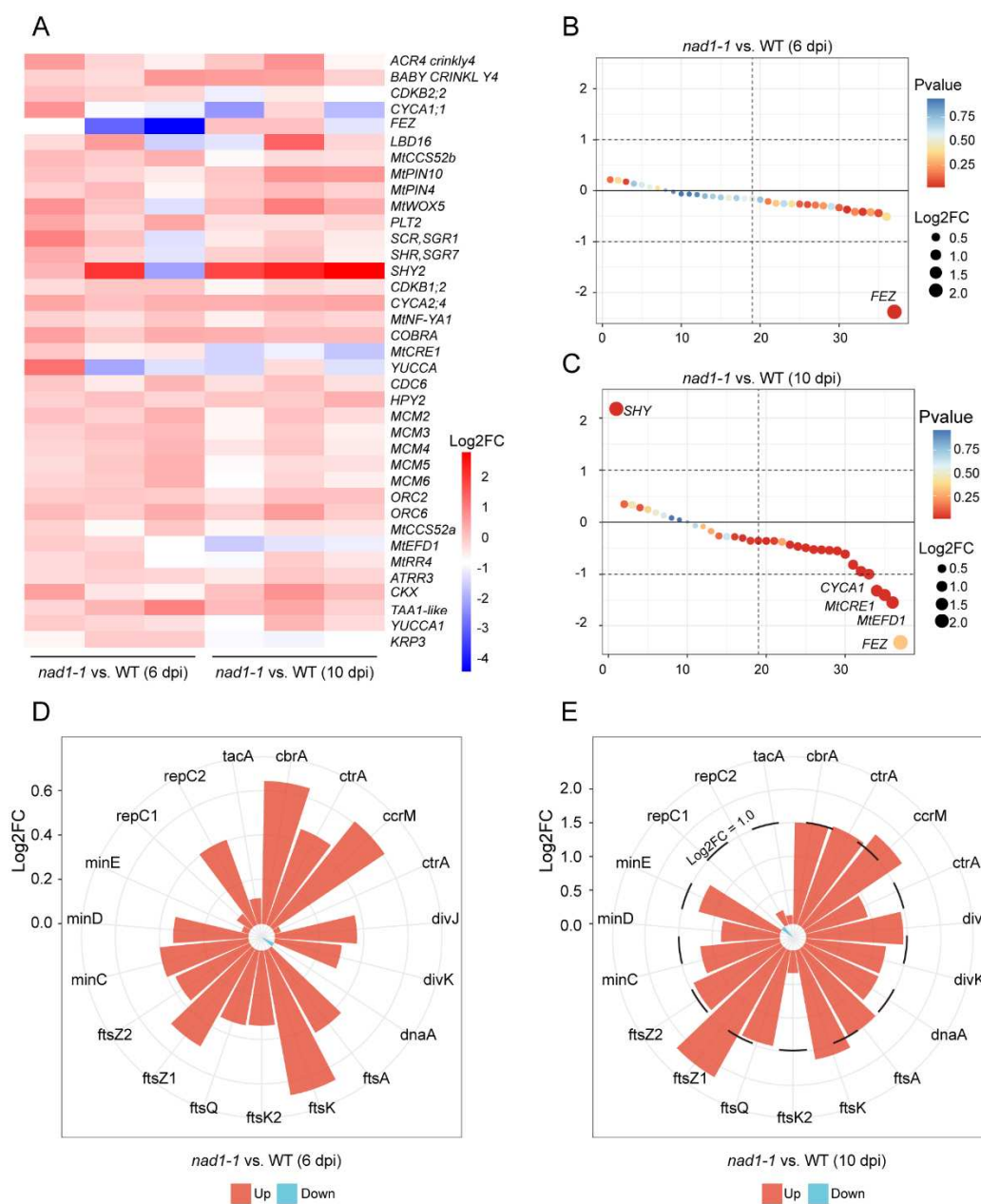


Figure 5. Candidate genes involved in the control of the nodule meristem and differentiation. A, Heatmap showing the transcriptional expression levels of all plant genes related to nodule meristem

and differentiation. B and C, Gene ranking dotplots showing the DEGs related to nodule meristem and differentiation between *nad1-1* and WT at 6 dpi (B) and 10 dpi (C) in *M. truncatula*. D and E, Rose charts showing the DEGs related to nodule meristem and differentiation at 6 dpi (D) and 10 dpi (E) in *S. meliloti*.

For rhizobia, the characteristic elongated bacteroid shape is associated with the change of rhizobial genes related to cell division during nodule differentiation [39]. Most bacterial genes involved in cell division (*ftsQAZ*, *ftsK*, and *minCDE*), initiation of DNA replication (*dnaA*, *repC1*, and *repC2*), and cell cycle control (*ctrA*, *cbrA*, *tacA*, *ccrM*, and *divJ*) exhibited no significant difference in the expression levels from those in wild type at 6 dpi (Figure 5D, Table S6). However, the expressions of the genes involved in cell division (*ftsA*, *ftsK*, *ftsQ*, *ftsZ1*, *ftsZ2*, *minC*, and *minE*), initiation of DNA replication (*dnaA*) and cell cycle control (*cbrA*, *tacA*, *ccrM*, *divJ*, and *cckA*) were significantly higher in *nad1-1* mutant than in wild type at 10 dpi (Figure 5E). The above data indicated that the *NAD1* is required for the transition of bacteria from active division to a state of cell differentiation, undergoing multiple rounds of endoreduplication without division.

2.6. Effects of *NAD1* gene on nodule symbiosis

During the developmental stage of nodule differentiation, a distinctive feature is the accumulation of specialized heme-containing proteins, such as leghemoglobins, which impart a pink color to the nitrogen-fixation zone. Leghemoglobins play a crucial role in creating microoxic conditions and are essential for nitrogenase activity and the maximal expression of *nif* genes. Our data showed that compared with wild-type, the *nad1-1* mutant exhibited significantly downregulated nitrogen fixation ability both at 6 dpi and 10 dpi (Figure 1C). In order to explore the role of *NAD1* in the interaction between plants and rhizobia, we examined the expressions of the genes related to nodule symbiosis (Figure 6A, 6B, Table S7) [10]. Clusters of symbiotic genes, such as leghemoglobin, NCR genes, CaM-like genes are most highly expressed in the nitrogen-fixation zone, the interzone II-III, or within infected cells of the nitrogen-fixation zone in wild-type nodules during the late stage of nodule development [25]. Remarkably, our data showed the expression levels of leghemoglobin, NCR and CaM-like genes were significantly down-regulated at both 6 dpi and 10 dpi between *nad1-1* and wild-type (Figure 6B). This is related to the serious defect of nitrogen fixation activity in *nad1-1* mutants. Flavonoids act as signal molecules during symbiotic interaction between legume and the rhizobia, which is essential for nodulation. Flavone synthase II (*FNSII*), a key enzyme responsible for flavonoid biosynthesis, is related to the number of nodules [40]. Our data showed that *FNSII* was upregulated at both 6dpi and 10dpi (Figure S1B) Four genes including *MtPEN-like*, *MtCPK3*, and *MtZPT2-1* were significantly up-regulated at both 6dpi and 10dpi (Figure S1A, S1B). These results may be explained the phenotype of increased number of nodules in the *nad1-1* mutant [23,41].

As for rhizobia, a striking feature in nitrogen-fixing is expression of nitrogenase structural genes (*nif*). In *Sinorhizobium spp.*, *nif* gene expression is regulated by the FixL/J-oxygen sensing system and NifA transcriptional activator under microoxic conditions [42]. Among the identified *nif* genes, *nifA* is the positive regulator of most *nif* and *fix* genes, and it is also regulated by *fixL* and *fixJ* genes and the products of oxygen partial pressure. *nifHDK* are the structural gene of nitrogenase, which is highly conserved in all nitrogen-fixing microorganisms and is activated by NifA. *FixL* and *fixJ* are a pair of regulator genes, and they can induce *nifA* and *nifK* gene expression and regulate symbiotic nitrogen fixation in root nodules through these two genes [43].

We observed significant changes in *nif* and *fix* gene expressions during nodule development (Figure 6C, Table S8). The expressions of six colocalized chromosomal genes (*fixs2*, *fixO3*, *fixI2*, *fixQ3*, *fixP3*, and *fixN3*) were significantly higher in *nad1-1* mutant nodules than in wild-type nodules at 6dpi and 10dpi (Figure 6C), which was different from the down-regulated expression pattern in the *dnf* mutant [42]. Iron-sulfur cluster assembly gene *nifS* exhibited a higher expression in *nad1-1* mutant nodules than in R108 nodule (Figure 6C), which suggested that *NAD1* might be involved in the formation of the nitrogen-fixation nodule. Moreover, half *nif* and *fix* genes (20 out of 40) exhibited lower expression in *nad1-1* mutant nodules than in R108 nodules (Figure 6C). The expression levels

of these nitrogen-fixing genes were consistent with the phenotype of the *nad1-1* mutant that cannot fix nitrogen.

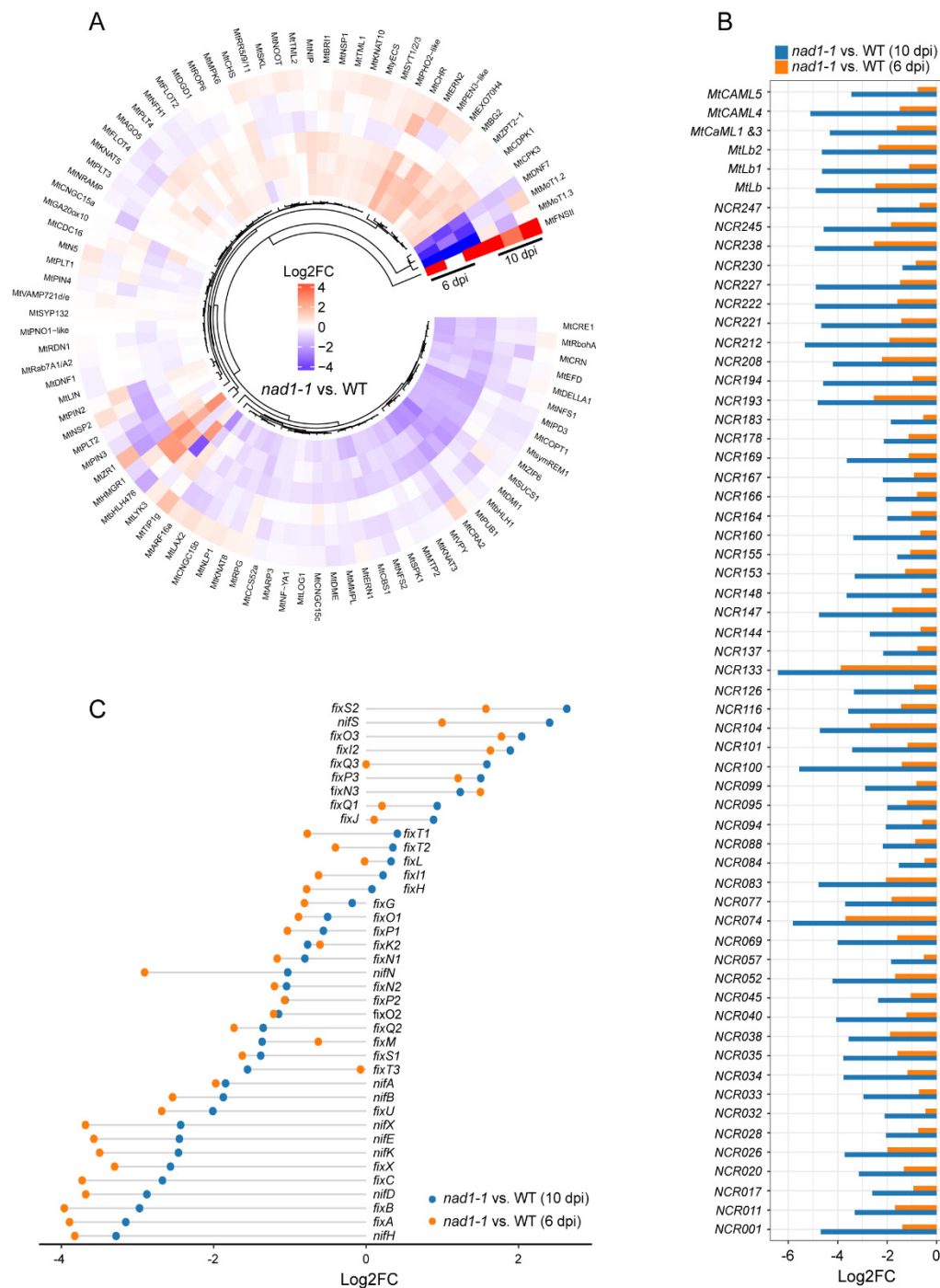


Figure 6. Identification of plant and rhizobial transcriptional responses in symbiotic nitrogen fixation processes. A, Heatmap showing relative expression levels for the genes in symbiotic nitrogen fixation processes in *M. truncatula*. B, Barlot showing expression profiles of leghemoglobin, NCR, and CaM-like genes in *M. truncatula*. D, Dotchart plot showing expression profiles of *nif* and *fix* genes in *S. meliloti*.

2.7. Interactome Analysis of *Medicago* and *Sinorhizobium* During Defense

In order to reveal the role of *NAD1* in the interaction between plants and rhizobia, we investigated the expressions of the genes related to plant immune signals (Figure 7C, Table S9) at 6 dpi and 10 dpi. We identified 98 genes as plant immunity-related ones in *nad1-1* nodules, of which 10 genes were up-regulated and 18 genes were down-regulated in *nad1-1* mutant at 6 dpi (Figure 7A). At 6 dpi, the plant defense response was slightly induced in *nad1-1* mutant. At 10 dpi, 64 genes and 25 genes were up-regulated and down-regulated in *nad1-1* mutant, respectively, and the plant defense response was significantly induced (Figure 7B). Furthermore, well-known marker genes related to defense such as *PR10* and *NDR1* were up-regulated at 6 dpi or 10 dpi (Figure 7A, 7B, 7C) and the genes involved in suppression of plant defense in nodules such as *DNF2*, *SymCRK*, and *RSD* were down-regulated in *nad1-1* mutant at 10 dpi, but their expressions exhibited little change at 6 dpi (Figure 7C).

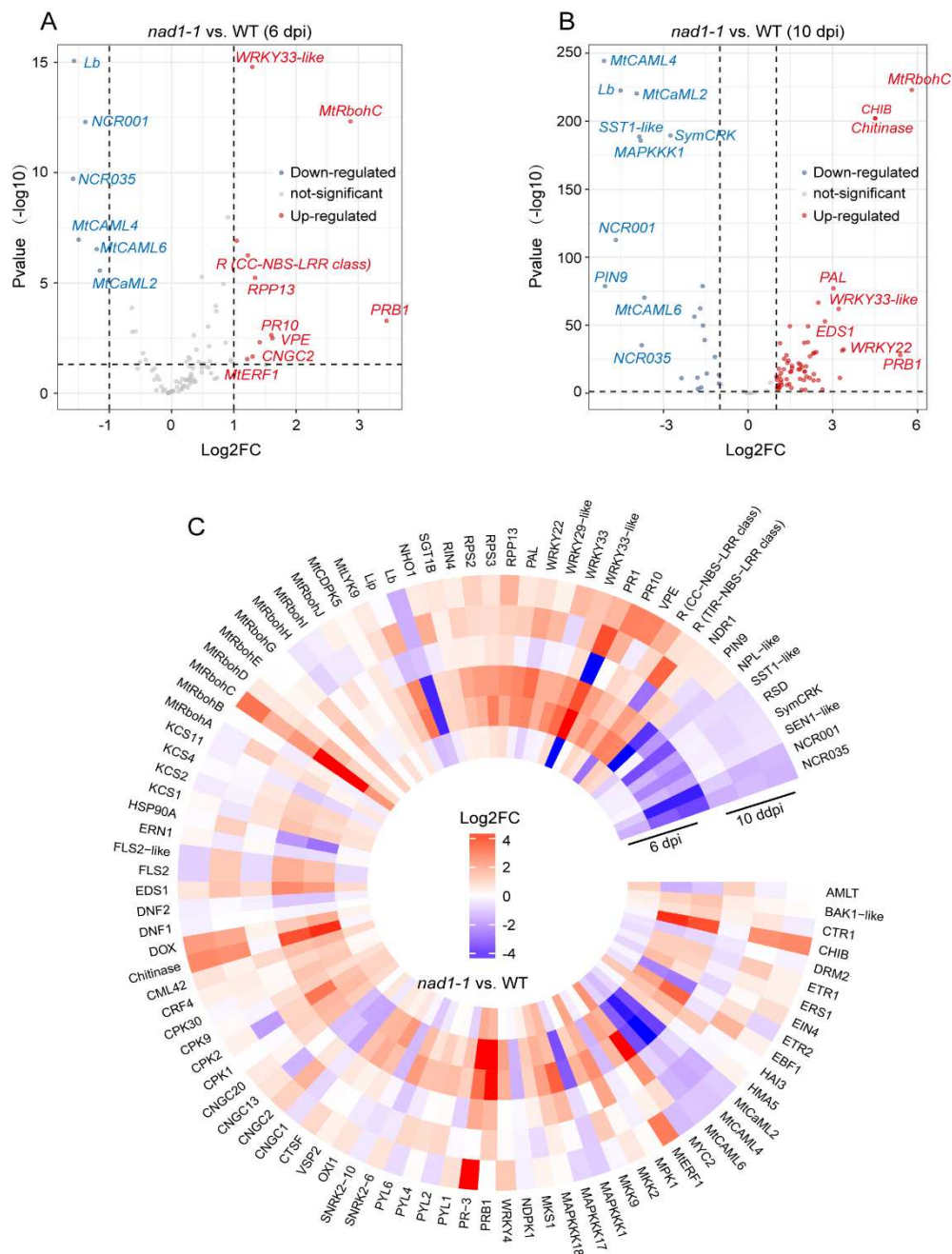


Figure 7. Transcriptomic analysis of *M. truncatula* gene expression during defense. A and B, Volcano plots showing differential expression of defense genes in *nad1-1* vs. WT at 6 dpi (A) and 10 dpi (B).

The top 10 genes ordered by log₂ fold change are highlighted, and genes with an adjusted p-value of < 0.05 are considered statistically significant. C, Heatmap showing relative expression levels of defense-related genes in plant at 6 dpi and 10 dpi in *nad1-1* vs. WT.

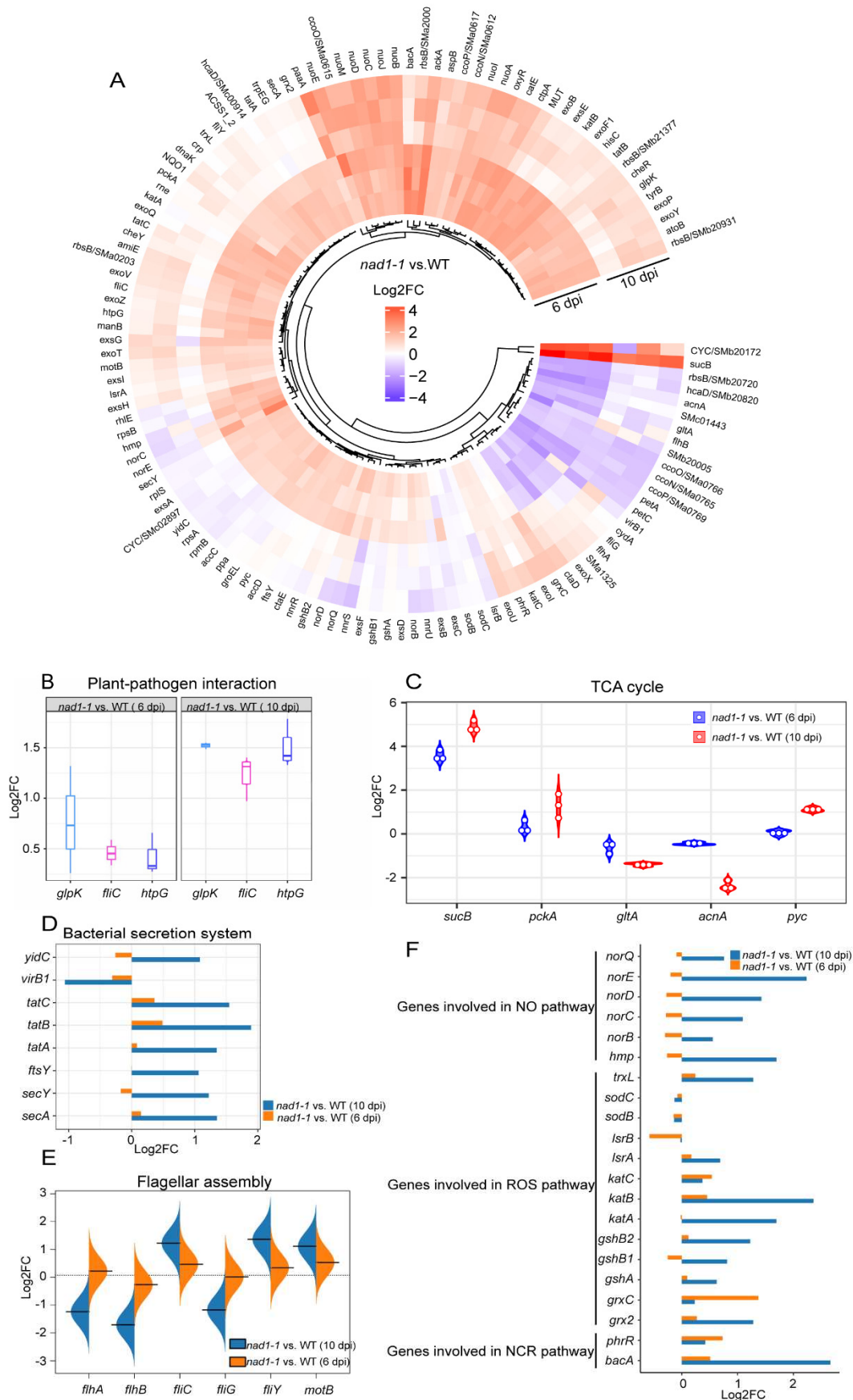
Genes involved in PAMP perception such as LRR-receptor kinase (*FLS2*, *BAK1*) and LysM-receptor kinase (*MtLYK9*) showed no significant expression difference between *nad1-1* mutant and wild-type at 6dpi, but their expression was significantly upregulated at 10 dpi in *nad1-1* mutant (Figure 7C). Similarly, the genes related to NADPH oxidases (*MtRbohD* and *MtRbohG*), calcium channel (*CPK1*, *CPK2*, *CPK9*, *CPK30*, *CNGC1*, *CNGC2*, *CNGC13*, and *CNGC20*), MAPK pathway (*MKK2*, *MKK9*, *MAPKKK1*, *MAPKKK17*, and *MAPKKK18*) and WRKY transcription factors (*WRKY4*, *WRKY22*, *WRKY29-like*, and *WRKY33*) displayed little alteration at 6 dpi, but they were remarkably upregulated at 10 dpi in *nad1-1* mutant, compared with those in wild-type (Figure 7C). Taken together, these data indicated that *NAD1* transcriptome switched from symbiosis to defense-related processes.

To reveal the response of rhizobia to the strong defense of *nad1-1* mutant plant, we investigated the expression of the genes involved in exopolysaccharide (EPS) synthesis and host defense suppression (*exoB*, *exoF*, *exoP*, *exoQ*, *exoV*, *exoY*, *exoZ*, *exsA*, *exsE*, and *exsG*) in the interactions between *M. truncatula* and *S. meliloti* [44]. The results showed that the expression of these genes showed no significant difference between *nad1-1* mutant and the wild-type at 6 dpi, but their expressions were up-regulated at 10 dpi (Figure 8A, Table S10).

In plant-pathogen interaction pathway, glycerol kinase-encoding *glpK* [45] and high temperature protein G-encoding *htpG* [46] can influence the nodule development and nitrogen fixation. In this pathway, *glpK* and *htpG* exhibited a higher expression level in *nad1-1* mutant than in wild-type at 10 dpi (Figure 8B). Tricarboxylic acid cycle (TCA cycle) plays a central role in maintaining bacterial metabolic status [47], and TCA cycle-related gene expression may change in *nad1-1* mutants. Consistent with this previous report, our results indicated that *sucB* encoding malate dehydrogenase in TCA cycle was significantly up-regulated at both 6 dpi and 10 dpi (Figure 8C). Furthermore, TCA cycle-related genes (*gltA*, *acnA*, and *pyc*) exhibited higher expression levels in *nad1-1* mutant at 10 dpi (Figure 8C). Based on these findings, the high expression levels of TCA-cycle genes in *nad1-1* mutant nodules of defective nitrogen-fixation suggest that the rhizobia have access to plant-derived carbon sources, even though they do not efficiently fix nitrogen, which is consistent with previous research [42].

Bacterial secretion system is important for the virulence of many animal and plant pathogenic bacteria, and rhizobial secretion system can secrete effectors to modulate their host specificity and symbiotic efficiency [16]. *SecA* and *SecY* are conserved and essential proteins for all bacteria, which are peripheral membrane ATPases which are involved in pre-protein translocation and integrated into the cellular membrane in bacteria [48]. Genes (*tatA*, *tatB*, and *tatC*) encoding translocase protein in *SecA*- and *SecY*- independent manner are required for symbiotic nitrogen fixation and aspartate catabolism [49]. Our data showed that the genes related to protein transport mentioned above were significantly higher in *nad1-1* mutant than in wild-type at 6 dpi and 10 dpi (Figure 8D), and that the expression of *virB1*, a component of type IV secretion system, was down-regulated at both 6 dpi and 10 dpi (Figure 8D).

Since flagellar assembly is crucial for the rhizobium motility, and it can influence the nodulation [50], we examined the expression of flagella-related genes to explore the mobility of rhizobia. The results showed, the expressions of flagellar assembly genes (*flhA*, *flhB*, *fliC*, *fliG*, *fliY*, and *motB*) showed little difference between *nad1-1* mutant and wild-type at 6 dpi, but genes (*flhA*, *flhB*, *fliG*) and genes (*fliC*, *fliY*, *motB*) were remarkably downregulated and upregulated at 10 dpi (Figure 8E), respectively.



the TCA cycle pathway. D and F, Bar plots showing relative expression levels for genes in the bacterial secretion system (D), NO, ROS and NCR pathways (F). E, Bean plot showing expression levels of genes involved in the flagellar assembly.

Bacteria are exposed to different environmental stresses including ROS and reactive nitrogen species during legume-rhizobial symbiosis [16]. The microsymbionts containing a large number of antioxidants and ROS-scavenging enzymes can protect the bacteroids against NO and ROS damages [42,16,51,52]. Genes enriched in NO pathway (*norBCD*, *norE*, *norQ*, and *hmp*) and ROS pathway (*trxL*, *katA*, *katB*, *gshA*, *gshB*, and *grx2*) displayed higher expression in *nad-1* mutant than wild-type at 6dpi and 10 dpi (Figure 8F).

NCR peptides have been specifically found in the inverted repeat-lacking clade (IRLC) legumes, and they target symbiosomes, affecting bacterial growth and inducing bacteroid morphological changes [42,51]. To survive, *S. meliloti* exposed to toxic NCR peptides requires the integrity of the BacA ABC-transporter [51]. Our results showed that the gene expression of *bacA* was significantly upregulated in *nad1-1* mutant at 10dpi (Figure 8F). Taken together, these data indicated that rhizobia responded to the plant immunity stress by regulating related gene expressions.

3. Discussion

In this study, we found that in addition to previously reported role in maintaining rhizobial endosymbiosis during nodulation [22], *NAD1* also functioned in the early-stage nodule development and symbiotic nitrogen fixation. Our phenotype observation showed at 6 dpi, symbionts remained in the infection zone of *nad1-1* mutant nodules (Figure 1D). In the nitrogen fixation zone, symbiotic cells ruptured, and many rhizobia were released from the cells, but brown deposition was hardly observed. At 10 dpi, most of the symbiotic cells in the root nodules of the *nad1-1* mutant ruptured, which was accompanied by obvious brown deposition. Our dual RNA-seq data elucidated the important role of *NAD1* in plant-rhizobium interaction.

NF production and signal transduction take place not only in the nodule infection zone but also in nitrogen fixing zone which might be associated in particular with infection threads [35]. During the nodule meristem and differentiation stages of wild-type, the endosymbiosis requires the coordination of plants and rhizobia [35]. Our study data showed that at 6dpi, the expressions of the genes related to NF signaling and nodule meristem and differentiation displayed no difference between *nad1-1* mutant and wild-type (Figure 4, Figure 5), implying that *NAD1* had no effect on early-stage NF signaling and nodule meristem and differentiation, which is consistent with the spatio-temporal expression of *NAD1* [22].

As an extraneous microorganism, the invasion of rhizobia tends to trigger certain plant immunity. In the early-stage symbiotic interactions, the expression levels of some immune response genes in plants are upregulated, but these immune responses are gradually suppressed in subsequent symbiotic interactions [53]. Although rhizobia are required symbionts in nodules, they must actively suppress or escape from the plant innate immune system so as not to be identified as foes by hosts. As hosts, plants have evolved multiple strategies to regulate their own defense systems to allow rhizobial entry, colonization, and differentiation and nodule organogenesis [24]. Thus, a balanced immune response between legumes and rhizobia is required for the development of nitrogen-fixing nodules in plants.

In our study, the deletion of *NAD1* protein specifically triggered the immune response in the nodules, thus leading to the termination of rhizobia colonization and bacteroid development (Figure 1D, 1E), eventually breaking the balance between symbiosis and immunity in nodules. A slight defense reaction including the production of reactive oxygen species (ROS) and defensin-like antimicrobial compounds was observed in the *nad1-1* mutant, which was in line with expression change pattern of the defense-related genes (*PR10*, *NDR1*, R protein, *EDS1*, *MtRbohC*) at 6 dpi (Figure 8A). In this early-stage nodule development, the expressions of most genes related to symbiotic nitrogen fixation in plant exhibited no difference between *nad1-1* mutant and wild type. To escape from host defenses, the rhizobium-infected cells can passively protect themselves and actively

modulate host functions [16]. Although there was no significant difference in the immune-related rhizobial gene expression between *nad1-1* mutant and wild-type at 6 dpi, the *nif* and *fix* genes related to nitrogen fixation exhibited significant difference at this stage. One possible explanation is that defense is more likely to be a cause than a result of blocking nitrogen fixation.

The *nad1-1* mutant made a strong defense response at 10 dpi, which was in agreement with the observation that most of genes related to plant immunity and nitrogen fixation were significantly different between *nad1-1* mutant and wild-type. It has been reported that plants generate reactive oxygen species (ROS) as signaling molecules to participate in the legume-rhizobium symbiotic interaction [55]. Plant NADPH oxidase (NOX), also known as respiratory burst oxidase homolog (RBOH), is a key producer of reactive oxygen species (ROS) in plants. In our study, RBOHC in *nad1-1* mutant showed significant up-regulation, compared to that in wild-type group at both 6 dpi and 10 dpi, suggesting the involvement of MtrbohC-mediated ROS in defense responses in *nad1-1* mutant [35]. Furthermore, knocking out the MtrbohBCD gene in the *nad1-1* mutant can weaken the defense responses of nodules [34], further confirming that MtrbohBCD-mediated ROS is involved in the defense response in nodules.

ROS is produced throughout root nodule development, acting both as antimicrobial agents and signals for nodule organogenesis [55]. In the early phases of root nodule development, it is crucial to limit ROS levels, enabling the coexistence of rhizobia [55]. However, higher ROS levels can have a negative impact on the survival of rhizobia [22, 34]. The analysis of rhizobial mutants deficient in various components including glutathione synthetase (*gshB*) [56], thioredoxin (*trxL*) [57], glutaredoxins (*grx1*, and *grx2*) [58], superoxide dismutase (*sodA*) [59], and catalases (double mutants *katA/katC* or *katB/katC*) [60] revealed that alterations in antioxidant pools and mutations in ROS detoxification enzymes have a negative impact on nodule formation. Additionally, these mutants lead to a reduction in N₂-fixing capacity and the initiation of premature nodule senescence. Furthermore, nodules induced by a deletion mutant of *lsrB* in *S. meliloti*, which encodes a LysR transcription factor serving as a ROS regulator, exhibited premature senescence coupled with impaired bacteroid differentiation [51]. Our research reveals that the expression of ROS-related genes did not exhibit difference at 6dpi, but they were noticeably up-regulated at 10 dpi in *nad1-1* mutant (Figure 8F). This suggests that the rhizobia adjust the expression levels of ROS-related genes to counteract the damage caused by ROS generated by the plant defense.

Nitric oxide (NO) belongs to biologically active compounds and has been confirmed to participate in various stages of nodulation, including rhizobial infection, nodule development, senescence, and nitrogen-fixing ability [8]. NO may participate in regulating the activity of two N₂ fixation genes, *nifA* and *fixK*, by forming a complex with the membrane-bound protein FixL [8]. Increased NO level in nodule inhibits the expression of the rhizobial nitrogenase genes *nifD* and *nifH* [61]. Additionally, NO can also induce the cytokinin receptor *CRE1* [62]. Elevated levels of NO within nodules are obtained through the utilization of *S. meliloti* mutant strains (*hmp*, *norB*, *nnrS1*) with impaired NO degradation [63]. Conversely, via *S. meliloti* mutants overexpressing *hmp*, a reduction in NO levels was noted [64]. However, the balance of NO concentration between plants and rhizobia needs to be maintained to avoid its toxic effects, and its mechanisms during nodulation and nitrogen fixation processes remain unclear. Our study provides a detailed exploration of the expression levels of genes associated with NO, laying a theoretical foundation for subsequent research.

4. Materials and Methods

4.1. Growth and Inoculation of Plant cultivation, inoculation, and root-nodule harvest

Wild-type *Medicago truncatula* ecotype R108 and homozygous *nad1-1* mutants were employed for the phenotype analysis. Seeds were subjected to scarification in H₂SO₄ for 2 minutes, followed by sterilization with 2.5% active chlorine for 5–8 minutes. Surface-sterilized seeds were synchronized at 4°C in darkness for 2 days. Seeds were placed upside-down on N-free Fahraeus medium containing 1.2% agar, as specified in the *Medicago Handbook* (<http://www.noble.org/MedicagoHandbook/>). The growth experiments were conducted at 22°C in darkness for a duration of 12–16 hours to induce

hypocotyl elongation. Germinated seedlings, numbering between nine to twelve, were transplanted into 10 × 10 cm growth pots. These pots contained a perlite: vermiculite mixture in a 1:2 ratio and were supplied with half-strength Fahraeus medium. The plants were cultivated under controlled conditions with a day: night regime of 16 hours at 24°C and 8 hours at 18°C, maintaining a relative humidity of 40–60%. Following four days of growth, each plant was inoculated with 50 ml of *Sinorhizobium meliloti* 2011 suspension per pot. The inoculum was prepared to an optical density at OD₆₀₀ of 0.02. Liquid culture of *S. meliloti* 2011 was pelleted by centrifugation after overnight growth in Tryptone Yeast (TY) medium (OD₆₀₀= 1.0). The pellet was then resuspended in half-strength Fahraeus medium containing 0.5 mM KNO₃. Harvesting of R108 and *nad1-1* mutant nodules were conducted at 6 and 10 days post-inoculation. For the purpose of RNA sequencing (RNA-seq), three independent biological replicates were prepared.

4.2. Acetylene reduction assay

Nitrogenase activity of nodulated roots, detached from intact plants, was measured using the acetylene reduction activity (ARA) method. This involved incubating three to five roots with 2 ml of acetylene (C₂H₂) in a closed 40 ml vial at 28°C for 2 hours. Acetylene gas was generated by reacting CaC₂ (Sigma–Aldrich, CAS No.: 75-20-7) with H₂O and subsequently purified through filtration using a saturated CuSO₄ solution. A volume of one hundred microliters of gas from each vial was utilized to measure the ethylene content employing a GC-4000A gas chromatograph (Dongxi, Beijing, China). For each sample, at least 40 plants divided into ten replicates were analyzed. Nitrogenase activity was calculated by normalization to nodule fresh weight and/or per plant [35]. Statistical analysis was performed using GraphPad Prism version 6 with Students *t*-test; a probability value lower than 0.05 was deemed statistically significant.

4.3. Microscopy Analyses

For microscopy analysis, nodules were excised using a scalpel, allowing for slight trimming if necessary for aesthetics. The nodule surfaces were gently brushed clean using a small bristle brush. Then, harvested nodules were fixed using FAA (Servicebio Cat No.: G1103-500ML) fixative solution, subject to vacuum conditions for 30 minutes, followed by incubation at room temperature for 1-2 hours. Subsequently, the nodules were rinsed twice with phosphate buffer solution at pH 7.2, each time soaking for ten minutes.

The fixed nodules were dehydrated using a gradient of ethanol solutions (30%, 50%, 70%, and 100%). Each ethanol concentration was applied for 10-30 minutes, with three repetitions of the 100% ethanol step. The processed nodules were subjected to resin infiltration through the following procedure: sequential immersion in SolA with anhydrous ethanol ratios of 1:3, 1:1, and 3:1, each lasting 30 minutes to 1 hour, followed by a 1-hour immersion in SolA. SolA was composed of the following components: 100 ml of Technovit 7100 (KULZER No.: 6470003), 1 pack of Hardener I (KULZER No.: 6470003), and 2.5 ml of PEG400 (Sigma CAS No.: 25322-68-3). Following this, the nodules were carefully positioned in molds, with a capacity of 3 to 5 nodules per mold. The embedding solution was introduced gradually along the contours of the mold to prevent nodule displacement. Subsequently, the molds were securely covered with sealing film. Ultimately, the molds were positioned within a fume hood to facilitate solidification. The embedding solution was prepared through the combination of 15 ml of SolA and 1 ml of Hardener II (KULZER No.: 6470003), with this preparation procedure being performed on ice. Resin-embedded nodules were sectioned longitudinally into 5 μm slices using a HistoCore AUTOCUT (Leica, Wetzlar, Germany). Nodule sections were stained with toluidine blue at room temperature for 30 minutes, followed by multiple rinses with distilled water using a small amount of water vapor each time. Sections were observed and photographed using a light microscope (Nikon ECLIPSE 80i, Tokyo, Japan). Nodules were observed and photographed by a fluorescence stereo microscope (Olympus SZX16, Tokyo, Japan).

4.4. RNA Isolation/ RNA purification, amplification, and Sequencing

Total RNAs were isolated using the Yeasen RNeasy kit in accordance with the manufacturer's protocol. Isolated RNA samples were quality checked using an Agilent 2100 Bioanalyzer. Subsequently, an RNA-seq library was constructed and sequenced on an DNBSeq platform with paired-end reads at Huada (Shenzhen, China). About 14 Gb cleaned reads were obtained for each sample.

4.5. Dual RNA-seq Data analysis

Raw sequencing reads were analyzed using Fastp for quality control. Clean reads were mapped to the *M. truncatula* A17 genome (Mt20120830-LIPM) [36], and the *S. meliloti* genome GMI11495-Rm2011G.20130218.submit.genome.fna (<https://iant.toulouse.inra.fr/bacteria/annotation/site/tmp/WBjXPIZ0/GMI11495-Rm2011G.20130218.submit.genome.fna>) respectively. Alignment and quantification were conducted using the STAR software, leading to the generation of read count data. Read counts were then imported into R (<http://www.r-project.org/>, v.3.1.2) for normalization and differentially expressed transcripts (fold change ≥ 1 , P-value ≤ 0.05) were determined using DESEQ [65]. PCA analysis and visualization, GO enrichment analysis and visualization, KEGG enrichment analysis and visualization, as well as heatmap generation, were all carried out using R scripts.

5. Conclusions

In summary, our study revealed that *NAD1* plays a multifaceted role in the establishment of symbiotic interactions between plants and rhizobia. Apart from its previously reported function in maintaining rhizobial endosymbiosis during nodulation, our findings demonstrate that *NAD1* also contributes to early-stage nodule development and symbiotic nitrogen fixation. The *nad1-1* mutant exhibited distinct phenotypic characteristics, with symbionts remaining in the meristem zone at 6 dpi and subsequent rupture of symbiotic cells in the nitrogen fixation zone, accompanied by brown deposition. This disruption in symbiosis was attributed to the significant downregulation of *NAD1*-related genes, resulting in impaired nitrogen fixation activity. Our dual RNA-seq data shed light on the vital role of *NAD1* in plant-rhizobium interactions. Interestingly, the expression of genes related to nitrogen fixation and nodule meristem and differentiation showed no significant differences between the *nad1-1* mutant and wild-type at 6 dpi, implying that *NAD1* primarily affects later stages of symbiosis. The delicate balance between plant immunity and symbiosis was disrupted in the *nad1-1* mutant, triggering a defense response that led to termination of rhizobial colonization and bacteroid development. Reactive oxygen species (ROS) and NO, as important signaling molecules, were implicated in these responses. The upregulation of ROS-related genes and the involvement of MtRbohBCD-mediated ROS highlighted their role in plant defense. Nitric oxide's impact on nodule development and nitrogen fixation was also emphasized, underscoring its intricate regulatory role. Further investigations could delve into the detailed mechanisms by which *NAD1* modulates the balance between immunity and symbiosis, as well as the precise roles of ROS and NO in nodule development and function. Unraveling these complexities will provide deeper insights into the intricate interplay between legumes and rhizobia, ultimately enhancing our understanding of nitrogen fixation and opening avenues for improved symbiotic plant-microbe interactions in agricultural contexts.

Supplementary Materials: The following supporting information can be downloaded at the website of this paper posted on Preprints.org. Figure S1: Identification of plant transcriptional responses in symbiotic nitrogen fixation processes; Table S1: Annotated list of plant genes that are differentially expressed in *nad1-1* nodules relative to wild type nodules; Table S2: Annotated list of rhizobial genes that are differentially expressed in *nad1-1* nodules relative to wild type nodules; Table S3: Nodule-associated NF signaling-related genes in *M. truncatula*; Table S4: Nodule-associated NF signaling-related genes in *S. meliloti*; Table S5: Candidate genes involved in the control of the nodule meristem and differentiation in *M. truncatula*; Table S6: Candidate genes involved in the control of the nodule meristem and differentiation in *S. meliloti*; Table S7: Plant nodule genes involved in

symbiotic nitrogen fixation; Table S8: Expression of rhizobia genes involved in symbiotic nitrogen fixation; Table S9: List of plant genes involved in defense; Table S10: Expression of rhizobia genes involved in defense.

Author Contributions: Conceptualization, D. Z. and Y.C.; methodology, D.Z. and H.Y.; software, D.Z. and Q.W.; validation, D.Z., Q.W., Z.Y. and H.Y.; formal analysis, D.Z. and Y.Z.; resources, H.Y.; data curation, D.Z.; writing, D.Z., Y.C. and H.Y.; visualization, D.Z. and A.X.; supervision and project administration, Y.C.; funding acquisition, Y.C. and H.Y. All authors have read and agreed to the published version of the manuscript.

Funding: This research was funded by the National Natural Science Foundation of China (32090063 and 32000191), and a self-innovation project from the national laboratory (AML2023B01). H.Y. and Y.C. were supported by Baichuan and Longyun fellowship from the Huazhong Agricultural University, respectively.

Institutional Review Board Statement: Not applicable.

Informed Consent Statement: Not applicable.

Data Availability Statement: The data disclosed in this study can be accessed through the article or Supplementary Materials provided here.

Conflicts of Interest: The authors declare no conflict of interest.

References

1. Oldroyd, G.E.D.; Leyser, O. A plant's diet, surviving in a variable nutrient environment. *Science*. **2020**, *368*, eaba0196.
2. Guo, K.; Yang, J.; Yu, N.; Luo, L.; Wang, E. Biological nitrogen fixation in cereal crops: Progress, strategies, and perspectives. *Plant Commun.* **2023**, *4*, 100499.
3. Sprent, J.I.; James, E.K. Legume evolution: where do nodules and mycorrhizas fit in? *Plant Physiol.* **2007**, *144*, 575-81.
4. Larrainzar, E.; Villar, I.; Rubio M.C.; Pérez-Rontomé, C.; Huertas, R.; Sato, S.; Mun J.H.; Becana, M. Hemoglobins in the legume-Rhizobium symbiosis. *New Phytol.* **2020**, *228*, 472-484.
5. Timmers, A.C.; Soupène, E.; Auriac, M.C.; de Billy, F.; Vasse, J.; Boistard, P.; Truchet, G. Saprophytic intracellular rhizobia in alfalfa nodules. *Mol Plant Microbe Interact.* **2000**, *13*, 1204-1213.
6. Hirsch, A.M. Developmental biology of legume nodulation. *New Phytol.* **1992**, *122*, 211-237.
7. Sprent, J.I. Evolving ideas of legume evolution and diversity: a taxonomic perspective on the occurrence of nodulation. *New Phytol.* **2007**, *174*, 11-25.
8. Gyan'ko, A.K. Signaling Systems of Rhizobia (Rhizobiaceae) and Leguminous Plants (Fabaceae) upon the Formation of a Legume-Rhizobium Symbiosis (Review). *Prikl Biokhim Mikrobiol.* **2015**, *51*, 453-464.
9. Roy, S.; Liu, W.; Nandety, R.S.; Crook, A.; Mysore, K.S.; Pislariu, C.I.; Frugoli, J.; Dickstein, R.; Udvardi, M.K. Celebrating 20 Years of Genetic Discoveries in Legume Nodulation and Symbiotic Nitrogen Fixation. *Plant Cell.* **2020**, *32*, 15-41.
10. Mergaert, P.; Uchiumi, T.; Alunni, B.; Evanno, G.; Cheron, A.; Catrice, O.; Mausset, A.E.; Barloy-Hubler, F.; Galibert, F.; Kondorosi, A.; Kondorosi, E. Eukaryotic control on bacterial cell cycle and differentiation in the Rhizobium-legume symbiosis. *Proc Natl Acad Sci U S A.* **2006**, *103*, 5230-5235.
11. Meng, X.; Zhang, S. MAPK cascades in plant disease resistance signaling. *Annu Rev Phytopathol.* **2013**, *51*, 245-266.
12. Gómez-Gómez, L.; Boller, T. FLS2: an LRR receptor-like kinase involved in the perception of the bacterial elicitor flagellin in *Arabidopsis*. *Mol Cell.* **2000**, *5*, 1003-1011.
13. Miya, A.; Albert, P.; Shinya, T.; Desaki, Y.; Ichimura, K.; Shirasu, K.; Narusaka, Y.; Kawakami, N.; Kaku, H.; Shibuya, N. CERK1, a LysM receptor kinase, is essential for chitin elicitor signaling in *Arabidopsis*. *Proc Natl Acad Sci U S A.* **2007**, *104*, 19613-19618.
14. Qi, D.; Innes, R.W. Recent Advances in Plant NLR Structure, Function, Localization, and Signaling. *Front Immunol.* **2013**, *4*, 348.
15. Boscari, A.; Del Giudice, J.; Ferrarini, A.; Venturini, L.; Zaffini, A.L.; Delledonne, M.; Puppo, A. Expression dynamics of the *Medicago truncatula* transcriptome during the symbiotic interaction with *Sinorhizobium meliloti*: which role for nitric oxide? *Plant Physiol.* **2013**, *161*, 425-439.
16. Saeki, K. Rhizobial measures to evade host defense strategies and endogenous threats to persistent symbiotic nitrogen fixation: a focus on two legume-rhizobium model systems. *Cell Mol Life Sci.* **2011**, *68*, 1327-39.

17. Zamioudis, C.; Pieterse, C.M. Modulation of host immunity by beneficial microbes. *Mol Plant Microbe Interact.* **2012**, *25*, 139-150.
18. Feng, Y.; Wu, P.; Liu, C.; Peng, L.; Wang, T.; Wang, C.; Tan, Q.; Li, B.; Ou, Y.; Zhu, H.; Yuan, S.; Huang, R.; Stacey, G.; Zhang, Z.; Cao, Y. Suppression of LjBAK1-mediated immunity by SymRK promotes rhizobial infection in *Lotus japonicus*. *Mol Plant.* **2021**, *14*, 1935-1950.
19. Bourcy, M.; Brocard, L.; Pislariu, C.I.; Cosson, V.; Mergaert, P.; Tadege, M.; Mysore, K.S.; Udvardi, M.K.; Gourion, B.; Ratet, P. *Medicago truncatula* DNF2 is a PI-PLC-XD-containing protein required for bacteroid persistence and prevention of nodule early senescence and defense-like reactions. *New Phytol.* **2013**, *197*, 1250-1261.
20. Berrabah, F.; Bourcy, M.; Eschstruth, A.; Cayrel, A.; Guefrachi, I.; Mergaert, P.; Wen, J.; Jean, V.; Mysore, K.S.; Gourion, B.; Ratet, P. A nonRD receptor-like kinase prevents nodule early senescence and defense-like reactions during symbiosis. *New Phytol.* **2014**, *203*, 1305-1314.
21. Sinharoy, S.; Torres-Jerez, I.; Bandyopadhyay, K.; Kereszt, A.; Pislariu, C.I.; Nakashima, J.; Benedito, V.A.; Kondorosi, E.; Udvardi, M.K. The C₂H₂ transcription factor regulator of symbiosome differentiation represses transcription of the secretory pathway gene *VAMP721a* and promotes symbiosome development in *Medicago truncatula*. *Plant Cell.* **2013**, *25*, 3584-3601.
22. Wang, C.; Yu, H.; Luo, L.; Duan, L.; Cai, L.; He, X.; Wen, J.; Mysore, K.S.; Li, G.; Xiao, A.; Duanmu, D.; Cao, Y.; Hong, Z.; Zhang, Z. *NODULES WITH ACTIVATED DEFENSE 1* is required for maintenance of rhizobial endosymbiosis in *Medicago truncatula*. *New Phytol.* **2016**, *212*, 176-191.
23. Berrabah, F.; Ratet, P.; Gourion, B. Multiple steps control immunity during the intracellular accommodation of rhizobia. *J Exp Bot.* **2015**, *66*, 1977-85.
24. Yu, H.; Bao, H.; Zhang, Z.; Cao, Y. Immune Signaling Pathway during Terminal Bacteroid Differentiation in Nodules. *Trends Plant Sci.* **2019**, *24*, 299-302.
25. Gu, Y.; Zebell, S.G.; Liang, Z.; Wang, S.; Kang, B.H.; Dong, X. Nuclear Pore Permeabilization Is a Convergent Signaling Event in Effector-Triggered Immunity. *Cell.* **2016**, *166*, 1526-1538.
26. Nobori, T.; Velásquez, A.C.; Wu, J.; Kvitko, B.H.; Kremer, J.M.; Wang, Y.; He, S.Y.; Tsuda, K. Transcriptome landscape of a bacterial pathogen under plant immunity. *Proc Natl Acad Sci U S A.* **2018**, *115*, E3055-E3064.
27. Mahmood, K.; Torres-Jerez, I.; Krom, N.; Liu, W.; Udvardi, M.K. Transcriptional Programs and Regulators Underlying Age-Dependent and Dark-Induced Senescence in *Medicago truncatula*. *Cells.* **2022**, *11*, 1570.
28. Fagorzi, C.; Bacci, G.; Huang, R.; Cangioli, L.; Checucci, A.; Fini, M.; Perrin, E.; Natali, C.; DiCenzo, G.C.; Mengoni, A. Nonadditive Transcriptomic Signatures of Genotype-by-Genotype Interactions during the Initiation of Plant-Rhizobium Symbiosis. *mSystems.* **2021**, *6*, e00974-e00920.
29. Zhang, A.; Luo, R.; Li, J.; Miao, R.; An, H.; Yan, X.; Pang, Q. Arabidopsis Glutathione-S-Transferases *GSTF11* and *GSTU20* Function in Aliphatic Glucosinolate Biosynthesis. *Front Plant Sci.* **2022**, *12*, 816233.
30. Ugalde, J.M.; Lamig, L.; Herrera-Vásquez, A.; Fuchs, P.; Homagk, M.; Kopriva, S.; Müller-Schüssele, S.J.; Holuigue, L.; Meyer, A.J. A dual role for glutathione transferase U7 in plant growth and protection from methyl viologen-induced oxidative stress. *Plant Physiol.* **2021**, *187*, 2451-2468.
31. Saliba, E.; Primo, C.; Guarini, N.; André, B. A plant plasma-membrane H⁺-ATPase promotes yeast TORC1 activation via its carboxy-terminal tail. *Sci Rep.* **2021**, *11*, 4788.
32. Liu, Y.; Fan, W.; Cheng, Q.; Zhang, L.; Cai, T.; Shi, Q.; Wang, Z.; Chang, C.; Yin, Q.; Jiang, X.; Jin, K. Multi-omics analyses reveal new insights into nutritional quality changes of alfalfa leaves during the flowering period. *Front Plant Sci.* **2022**, *13*, 995031.
33. Jia, X.M.; Zhu, Y.F.; Hu, Y.; Zhang, R.; Cheng, L.; Zhu, Z.L.; Zhao, T.; Zhang, X.; Wang, Y.X. Integrated physiologic, proteomic, and metabolomic analyses of *Malus halliana* adaptation to saline-alkali stress. *Hortic Res.* **2019**, *6*, 91.
34. Yu, H.; Xiao, A.; Dong, R.; Fan, Y.; Zhang, X.; Liu, C.; Wang, C.; Zhu, H.; Duanmu, D.; Cao, Y.; Zhang, Z. Suppression of innate immunity mediated by the CDPK-Rboh complex is required for rhizobial colonization in *Medicago truncatula* nodules. *New Phytol.* **2018**, *220*, 425-434.
35. Roux, B.; Rodde, N.; Jardinaud, M.F.; Timmers, T.; Sauviac, L.; Cottret, L.; Carrère, S.; Sallet, E.; Courcelle, E.; Moreau, S.; Debelle, F.; Capela, D.; de Carvalho-Niebel, F.; Gouzy, J.; Bruand, C.; Gamas, P. An integrated analysis of plant and bacterial gene expression in symbiotic root nodules using laser-capture microdissection coupled to RNA sequencing. *Plant J.* **2014**, *77*, 817-837.
36. Barnett, M.J.; Long, S.R. The *Sinorhizobium meliloti* SyrM regulon: effects on global gene expression are mediated by *syra* and *nodD3*. *J Bacteriol.* **2015**, *197*, 1792-1806.

37. Mathesius, U.; Crespi, M.; Frugier, F. MtCRE1-dependent cytokinin signaling integrates bacterial and plant cues to coordinate symbiotic nodule organogenesis in *Medicago truncatula*. *Plant J.* **2011**, *65*, 622-633.
38. Jardinaud, M.F.; Fromentin, J.; Auriac, M.C.; Moreau, S.; Pecrix, Y.; Taconnat, L.; Cottret, L.; Aubert, G.; Balzergue, S.; Burstin, J.; Carrere, S.; Gamas, P. MtEFD and MtEFD2: Two transcription factors with distinct neofunctionalization in symbiotic nodule development. *Plant Physiol.* **2022**, *189*, 1587-1607.
39. Alunni, B.; Gourion, B. Terminal bacteroid differentiation in the legume-rhizobium symbiosis: nodule-specific cysteine-rich peptides and beyond. *New Phytol.* **2016**, *211*, 411-417.
40. Zhang, J.; Subramanian, S.; Zhang, Y.; Yu, O. Flavone synthases from *Medicago truncatula* are flavanone-2-hydroxylases and are important for nodulation. *Plant Physiol.* **2007**, *144*, 741-751.
41. Gargantini, P.R.; Gonzalez-Rizzo, S.; Chinchilla, D.; Raices, M.; Giammaria, V.; Ulloa, R.M.; Frugier, F.; Crespi, M.D. A CDPK isoform participates in the regulation of nodule number in *Medicago truncatula*. *Plant J.* **2006**, *48*, 843-856.
42. Lang, C.; Long, S.R. Transcriptomic Analysis of *Sinorhizobium meliloti* and *Medicago truncatula* Symbiosis Using Nitrogen Fixation-Deficient Nodules. *Mol Plant Microbe Interact.* **2015**, *28*, 856-868.
43. Li, Q.; Chen, S. Transfer of Nitrogen Fixation (*nif*) Genes to Non-diazotrophic Hosts. *Chembiochem.* **2020**, *21*, 1717-1722.
44. Janczarek, M. Environmental signals and regulatory pathways that influence exopolysaccharide production in rhizobia. *Int J Mol Sci.* **2011**, *12*, 7898-7933.
45. Ding, H.; Yip, C.B.; Geddes, B.A.; Oresnik, I.J.; Hynes, M.F. Glycerol utilization by *Rhizobium leguminosarum* requires an ABC transporter and affects competition for nodulation. *Microbiology (Reading)*. **2012**, *158*, 1369-1378.
46. Zhou, D.; Li, Y.; Wang, X.; Xie, F.; Chen, D.; Ma, B.; Li, Y. *Mesorhizobium huakuii* HtpG Interaction with nsLTP AsE246 Is Required for Symbiotic Nitrogen Fixation. *Plant Physiol.* **2019**, *180*, 509-528.
47. Sadykov, M.R.; Zhang, B.; Halouska, S.; Nelson, J.L.; Kreimer, L.W.; Zhu, Y.; Powers, R.; Somerville, G.A. Using NMR metabolomics to investigate tricarboxylic acid cycle-dependent signal transduction in *Staphylococcus epidermidis*. *J Biol Chem.* **2010**, *285*, 36616-36624.
48. Hu, J.; Akula, N.; Wang, N. Development of a Microemulsion Formulation for Antimicrobial SecA Inhibitors. *PLoS One.* **2016**, *11*, e0150433.
49. Watson, R.J.; Rastogi, V.K. Cloning and nucleotide sequencing of *Rhizobium meliloti* aminotransferase genes: an aspartate aminotransferase required for symbiotic nitrogen fixation is atypical. *J Bacteriol.* **1993**, *175*, 1919-1928.
50. Zheng, H.; Mao, Y.; Teng, J.; Zhu, Q.; Ling, J.; Zhong, Z. Flagellar-dependent motility in *Mesorhizobium tianshanense* is involved in the early stage of plant host interaction: study of an *flgE* mutant. *Curr Microbiol.* **2015**, *70*, 219-227.
51. Syska, C.; Brouquisse, R.; Alloing, G.; Pauly, N.; Frenedo, P.; Bosseno, M.; Dupont, L.; Boscardi, A. Molecular Weapons Contribute to Intracellular Rhizobia Accommodation Within Legume Host Cell. *Front Plant Sci.* **2019**, *10*, 1496.
52. Cabrera, J.J.; Sánchez, C.; Gates, A.; Bedmar, E.J.; Mesa, S.; Richardson, D.J.; Delgado, M.J. The nitric oxide response in plant-associated endosymbiotic bacteria. *Biochem Soc Trans.* **2011**, *39*, 1880-1885.
53. Cao, Y.; Halane, M.K.; Gassmann, W.; Stacey, G. The Role of Plant Innate Immunity in the Legume-Rhizobium Symbiosis. *Annu Rev Plant Biol.* **2017**, *68*, 535-561.
54. Marino, D.; Andrio, E.; Danchin, E.G.; Oger, E.; Gucciardo, S.; Lambert, A.; Puppo, A.; Pauly, N. A *Medicago truncatula* NADPH oxidase is involved in symbiotic nodule functioning. *New Phytol.* **2011**, *189*, 580-592.
55. Montiel, J.; Arthikala, M.K.; Cárdenas, L.; Quinto, C. Legume NADPH Oxidases Have Crucial Roles at Different Stages of Nodulation. *Int J Mol Sci.* **2016**, *17*, 680.
56. Harrison, J. Jamet, A.; Muglia, C.I.; Van de Sype, G.; Aguilar, O.M.; Puppo, A.; Frenedo, P. Glutathione plays a fundamental role in growth and symbiotic capacity of *Sinorhizobium meliloti*. *J Bacteriol.* **2005**, *187*, 168-174.
57. Castro-Sowinski, S.; Matan, O.; Bonafede, P.; Okon, Y. A thioredoxin of *Sinorhizobium meliloti* CE52G is required for melanin production and symbiotic nitrogen fixation. *Mol Plant Microbe Interact.* **2007**, *20*, 986-993.
58. Benyamina, S.M.; Baldacci-Cresp, F.; Couturier, J.; Chibani, K.; Hopkins, J.; Bekki, A.; de Lajudie, P.; Rouhier, N.; Jacquot, J.P.; Alloing, G.; Puppo, A.; Frenedo, P. Two *Sinorhizobium meliloti* glutaredoxins regulate iron metabolism and symbiotic bacteroid differentiation. *Environ Microbiol.* **2013**, *15*, 795-810.

59. Santos, R.; Hérouart, D.; Puppo, A.; Touati, D. Critical protective role of bacterial superoxide dismutase in rhizobium-legume symbiosis. *Mol Microbiol.* **2000**, *38*, 750-759.
60. Jamet, A.; Sigaud, S.; Van de Sype, G.; Puppo, A.; Hérouart, D. Expression of the bacterial catalase genes during *Sinorhizobium meliloti*-*Medicago sativa* symbiosis and their crucial role during the infection process. *Mol Plant Microbe Interact.* **2003**, *16*, 217-225.
61. Sánchez, C.; Gates, A.J.; Meakin, G.E.; Uchiumi, T.; Girard, L.; Richardson, D.J.; Bedmar, E.J.; Delgado, M.J. Production of nitric oxide and nitrosylhemoglobin complexes in soybean nodules in response to flooding. *Mol Plant Microbe Interact.* **2010**, *23*, 702-711.
62. Del Giudice, J.; Cam, Y.; Damiani, I.; Fung-Chat, F.; Meilhoc, E.; Bruand, C.; Brouquisse, R.; Puppo, A.; Boscari, A. Nitric oxide is required for an optimal establishment of the *Medicago truncatula*-*Sinorhizobium meliloti* symbiosis. *New Phytol.* **2011**, *191*, 405-417.
63. Blanquet, P.; Silva, L.; Catrice, O.; Bruand, C.; Carvalho, H.; Meilhoc, E. *Sinorhizobium meliloti* Controls Nitric Oxide-Mediated Post-Translational Modification of a *Medicago truncatula* Nodule Protein. *Mol Plant Microbe Interact.* **2015**, *28*, 1353-1363.
64. Cam, Y. Pierre, O.; Boncompagni, E.; Hérouart, D.; Meilhoc, E.; Bruand, C. Nitric oxide (NO): a key player in the senescence of *Medicago truncatula* root nodules. *New Phytol.* **2012**, *196*, 548-560.
65. Anders, S.; Huber, W. Differential expression analysis for sequence count data. *Genome Biol.* **2010**, *11*, R106.

Disclaimer/Publisher's Note: The statements, opinions and data contained in all publications are solely those of the individual author(s) and contributor(s) and not of MDPI and/or the editor(s). MDPI and/or the editor(s) disclaim responsibility for any injury to people or property resulting from any ideas, methods, instructions or products referred to in the content.